

half-life were 4.3×10^{10} years and 6.3×10^{10} years, respectively. The dotted line through the experimental points corresponds to a half-life of 5.0×10^{10} years.

CONCLUSIONS

The data show that the ratio, $\text{Sr}^{87}/\text{Rb}^{87}$, is directly related to the age of the pegmatite for which it is de-

termined. From the data presented, the half-life of Rb^{87} is calculated to be $(5.0 \pm 0.2) \times 10^{10}$ years. It is important that this value be confirmed by laboratory counting experiments.¹³

¹³ Subsequent to submission of this paper, E. Huster and W. Rausch (private communication) reported that refined experiments of the type described in footnote g of Table I now give $(4.9-5.0) \times 10^{10}$ years for the half-life of Rb^{87} .

Analysis of Proton-Proton Scattering Data at 300 Mev*

M. H. HULL, JR.,† J. B. EHRLMAN,‡ R. D. HATCHER,§ AND L. DURAND†
Yale University New Haven, Connecticut, and New York University, New York, New York
 (Received March 26, 1956)

An analysis of proton-proton scattering experiments is described and some results for 300 Mev are presented. Phase shifts for states with $J \leq 4$ are included, and effects of states of higher angular momentum are discussed. The importance of including Coulomb interference effects is brought out.

INTRODUCTION

NUCLEON-NUCLEON interactions derived from meson field theories are not yet entirely satisfactory. Not only is the most hopeful one so far obtained apparently inadequate for explaining low-energy phenomena,¹ but the possibility of an as yet unknown velocity dependence of the interaction also makes it desirable to be able to approach the problem of interpretation of experimental data at high energies from some other viewpoint. The alternative approach is supplied by an analysis in terms of phase shifts, which Breit has shown to be valid² regardless of the possible radial, angular, or velocity dependence of the nucleon-nucleon potential or whether such a potential can even be logically defined.

In the present note, an account is given of a phase shift analysis of the data on proton-proton differential cross section and polarization at 300 Mev, and some preliminary results of the analysis are presented and discussed. The methods used do not involve the usual gradient search high-speed digital machine procedure, but rely on another type of search for fits to the differential cross section and an Argand diagram treatment of polarization data. These possibilities have been pointed out to the authors by Breit. No set of phase shifts has yet come out of the analysis which produces an unqualified fit to these data, but some results appear of sufficient interest to merit mention and to warrant a

description of the methods used to obtain them. In addition, the calculations are in a stage where statements can be made concerning effects of Coulomb interference and effects of phase shifts for states of higher angular momentum than are included in the analysis.

The high-energy polarization data³ have an angular dependence which implies phase shifts in the $J \geq 3$ states of total angular momentum,⁴ and the existence of polarization implies that the phase shifts for given orbital angular momentum state L but different J are unequal.⁵ If it is assumed that states for $L > 3$ are not important at 300 Mev, then the analysis of polarization and differential cross section is in terms of eight phase shifts: the singlets K_0 , K_2 , and the triplets δ_1^P , δ_1^F , δ_2^P , δ_2^F , δ_3^F , δ_4^F . If a tensor type interaction occurs, then the coupling parameter between the 3P_2 and 3F_2 states is a ninth parameter. Since the polarization involves only the triplet states, it was the subject of the first analysis and the cross-section data were treated afterwards.

II. PROCEDURE AND RESULTS

The following procedure, suggested by Breit,⁶ was followed in analyzing the polarization data. Coupling in the $J=2$ state was omitted, and values of scattering angle, θ , for which the Coulomb-nuclear interference effects should be negligible were investigated first. A least squares analysis of $(P\sigma) = \sin\theta [a_1 P_1(\cos\theta)]$

* This research was supported by the Office of Ordnance Research, U. S. Army.

† At Yale University, New Haven, Connecticut

‡ Now at Nucleonics Division, Naval Research Laboratory, Washington, D. C.

§ At New York University, New York, New York.

¹ J. M. Blatt and M. H. Kalos, *Phys. Rev.* **92**, 1563 (1953).

² G. Breit, *University of Pennsylvania Bicentennial Conference* (University of Pennsylvania Press, Philadelphia, 1941).

³ Chamberlain, Donaldson, Segrè, Tripp, Wiegand, and Ypsilantis, *Phys. Rev.* **95**, 850 (1954); J. M. Dickson and D. C. Salter, *Nature* **173**, 946 (1954).

⁴ B. D. Fried, *Phys. Rev.* **95**, 851 (1954); Breit, Ehrman, Saperstein, and Hull, *Phys. Rev.* **96**, 807 (1954).

⁵ G. Breit and J. B. Ehrman, *Phys. Rev.* **96**, 805 (1954); M. H. Hull, Jr., and A. M. Saperstein, *Phys. Rev.* **96**, 806 (1954).

⁶ G. Breit (private communication).

$+a_3P_3(\cos\theta)+a_5P_5(\cos\theta)]$ (excluding interference effects) in the angular range $25^\circ \leq \theta \leq 90^\circ$ was carried out to determine the coefficients a_1 , a_3 , and a_5 . Several sets of data⁷ were included, and the result is

$$a_1 = 1.015 \pm 0.057; \quad a_3 = 0.316 \pm 0.069; \quad a_5 = 0.099 \pm 0.073.$$

The large uncertainty in a_5 has already been discussed by Breit, Ehrman, Saperstein, and Hull.⁴ Even though the value of a_5 is uncertain it is used below since its omission might lead to erroneous conclusions. Formulas for the a 's in terms of phase shifts⁵ were then used, together with the least squares values, to determine sets of 3P and 3F phase shifts consistent with the polarization data. Only sets of triplet phase shifts such that $(4\pi/k^2) \sum_{L=1,3; J=0,\dots,4} (2J+1) \sin^2 \delta_J^L \leq \sigma_{\text{total}}$ were accepted. The total p - p cross section could be taken to be $4\pi \times \sigma_{p-p}(90^\circ) = 4\pi \times 3.75$ mb from the data of Chamberlain *et al.*⁸ In order not to restrict unduly the ranges of phase shifts investigated, 4 mb was used in place of 3.75 mb.

Trial values of δ_2^F , δ_3^F , and δ_2^P were chosen, and the least squares values of the coefficients a were used to determine δ_4^F , δ_0^P , and δ_1^P . Since a_5 depends only on the 3F phase shifts, selection of δ_2^F and δ_3^F determines δ_4^F from the value of a_5 . The phase shifts δ_0^P , δ_1^P enter in a_1 , a_3 only in the combination $Q_0^P + \frac{3}{2}Q_1^P \equiv \exp(i\delta_0^P) \times \sin \delta_0^P + \frac{3}{2} \exp(i\delta_1^P) \sin \delta_1^P$, and it is convenient therefore to introduce

$$x = \text{Re}(Q_0^P + \frac{3}{2}Q_1^P), \quad y = \text{Im}(Q_0^P + \frac{3}{2}Q_1^P).$$

With the selected values of δ_3^F , δ_4^F , δ_2^P , a_1 , a_3 , and a_5 , real values of δ_0^P and δ_1^P correspond to the condition

$$(\frac{1}{4})^2 \leq x^2 + [y - (5/4)]^2 \leq (5/4)^2.$$

Graphical methods were used for making use of these inequalities in many cases according to the following plan. One notes that

$$(9/25)a_5 = \text{Im}[(20Q_2^F + 7Q_3^F)(Q_4^F)^*].$$

On an Argand diagram, the points representing $(20Q_2^F + 7Q_3^F)(Q_4^F)^*$ for given δ_2^F and δ_3^F lie on a circle passing through the origin with radius $\frac{1}{2}|20Q_2^F + 7Q_3^F|$, and with a diameter which passes through the origin at an angle $\arg(20Q_2^F + 7Q_3^F)$ measured counterclockwise from the negative imaginary axis. The intersections of the line giving the experimental value of $\text{Im}[(20Q_2^F + 7Q_3^F)(Q_4^F)^*] = (9/25)a_5$ with the circle give the values of δ_4^F which are desired: they are the angles measured clockwise from the line through the origin at angle $\arg(20Q_2^F + 7Q_3^F)$ with respect to the positive real axis, to lines joining the origin with the

points of intersection. The sum of the two solutions must be $\arg(20Q_2^F + 7Q_3^F)$ regardless of the value of a_5 .

In order to obtain δ_0^P and δ_1^P , the values of x and y were calculated from values of δ_2^F , δ_3^F , δ_4^F , and an assumed value of δ_2^P . Thus, defining

$$\begin{aligned} \alpha &= a_1 - (27/25)a_5 - (21/2)(F_2, F_3) + (81/2)(F_2, F_4) \\ &\quad - 15(F_2, P_2) - (21/2)(F_3, P_2) + (51/2)(F_4, P_2), \\ \beta &= a_3 - (38/25)a_5 - (21/2)(F_2, F_3) + (81/2)(F_2, F_4) \\ &\quad - 30(F_2, P_2) - (21/2)(F_3, P_2) + (11/2)(F_4, P_2). \end{aligned}$$

one finds

$$\begin{aligned} x &= \frac{(\alpha/6) \text{Re}Q_4^F - (\beta/14) \text{Re}(Q_4^F - Q_2^F + Q_2^P)}{\text{Im}[Q_4^F(Q_2^P - Q_2^F)^*]}, \\ y &= \frac{(\alpha/6) \text{Im}Q_4^F - (\beta/14) \text{Im}(Q_4^F - Q_2^F + Q_2^P)}{\text{Im}[Q_4^F(Q_2^P - Q_2^F)^*]}, \end{aligned}$$

where

$$\begin{aligned} (L_J, L_{J'}) &\equiv \text{Im}(Q_J^L Q_{J'}^{L'*}) \\ &= \sin \delta_J^L \sin \delta_{J'}^{L'} \sin(\delta_J^L - \delta_{J'}^{L'}). \end{aligned}$$

If these satisfied the criterion for real δ_0^P and δ_1^P , then the values of the angles themselves were found graphically. Since $x + iy = Q_0^P + \frac{3}{2}Q_1^P$, the diagram consists of a circle of radius $\frac{3}{4}$ centered at $\frac{3}{4}i$, and a circle of radius $\frac{1}{2}$ centered at $x + i(y - \frac{1}{2})$. The intersections of these circles provide two pairs δ_0^P , δ_1^P . Here δ_1^P is the angle measured from the real axis to the line joining the origin with either intersection, and δ_0^P is the angle measured from the real axis to the line joining that intersection with the point $x + iy$.

Much of the effort in applying this method is involved in finding values of δ_2^P so that x , y yield real δ_0^P , δ_1^P when δ_2^F , δ_3^F have been selected and δ_4^F determined. It was usually found desirable to calculate x and y as functions of δ_2^P and from graphs of these quantities to restrict the investigation to regions where the necessary (but not sufficient) conditions $|x| < 5/4$, $0 < y < 5/2$ were satisfied. Approximate analytical methods were used for $|\delta_4^F|$ small ($\sim 1^\circ$) and for $\delta_2^P \sim \delta_2^F$ (where x and y diverge). It was found that only a small range ($< 5^\circ$ usually) of values of δ_2^P gave allowed values of x and y for small $|\delta_4^F|$, and usually the region containing $\delta_2^P = \delta_2^F$ was excluded.

The effect of experimental uncertainties, as contained in the results of the least squares analysis, was looked into by using the central and one of the extreme values of a_5 indicated by the analysis: $a_5 = 0.099$ and $a_5 = 0.172$. These changes in a_5 have little effect on the polarization curve, but do affect the ranges of allowed 3F phase shifts: generally smaller 3F phase shifts are allowed by smaller a_5 , and vice versa. The effect of uncertainties in the other coefficients was not investigated in this preliminary work, since on the percentage basis they were much smaller than for a_5 . It should be noted, however, that values of phase shifts obtained by this

⁷ Chamberlain, Donaldson, Segrè, Tripp, Wiegand, and Ypsilantis, Phys. Rev. **95**, 850 (1954); Chamberlain, Segrè, Tripp, Wiegand, and Ypsilantis, Phys. Rev. **93**, 1430 (1954); Chamberlain, Pettengill, Segrè, and Wiegand, Phys. Rev. **95**, 1348 (1954); Marshall, Marshall, and Carvalho, Phys. Rev. **93**, 1431 (1954).

⁸ Chamberlain, Pettengill, Segrè, and Wiegand, Phys. Rev. **95**, 1348 (1954); **93**, 1424 (1954).

method are sensitive to the measurement of the angles in the graphical method.

The principal errors arise from uncertainties in determining δ_4^F , where the scale of the construction sometimes made it necessary to find the intersections of a circle of large radius with a line a very small distance from zero. As an example, when fitting $a_5=0.099$ assuming $\delta_2^F=10^\circ$, $\delta_3^F=-5^\circ$, one finds that the radius of the circle is 1.44, and the angle with the vertical axis of the diameter passing through zero is only 13.13° . The intersections of this circle with a horizontal line only 0.035 above the horizontal axis had to be determined, and the larger of the two angles was measured as $\delta_4^F=8.3^\circ$, with an estimated error of reading and construction of the order of 1° . The smaller range was determined by subtraction to be $\delta_4^F=4.8^\circ$. This case was redone numerically, and the angle found to be 5.01° , so that the error in this case was rather small. With $\delta_4^F=4.8^\circ$, solutions for δ_0^P and δ_1^P were found for $\delta_2^P=21^\circ$. One finds $x=-0.5603$, $y=0.3156$, which lead to $\delta_0^P=-33.6^\circ$, $\delta_1^P=-4.1^\circ$. Using $\delta_4^F=5.01^\circ$, $\delta_2^P=21^\circ$, one finds $x=-0.5806$, $y=0.2981$ and corresponding phase shifts $\delta_0^P=-26.0^\circ$, $\delta_1^P=+1.5^\circ$. Since the scale of construction is always the same for the 3P phase shifts, the uncertainties which interfere with a precise graphical determination of the 3F_4 phase shift are not present, the changes coming almost entirely from the changes in x and y . The coefficients are not exceedingly sensitive to errors in the 3P phase shifts, even as large as those shown here. Thus for $\delta_4^F=4.8^\circ$, $\delta_3^F=-5^\circ$, $\delta_2^F=10^\circ$, $\delta_2^P=21^\circ$, $\delta_1^P=-4.1^\circ$, $\delta_0^P=-33.6^\circ$, one finds that $a_5=0.097$, $a_3=0.319$, $a_1=1.017$. In this case, therefore, the errors $\Delta a_5=-0.002$, $\Delta a_3=+0.003$, $\Delta a_1=+0.002$ are much less than the errors in the least squares analysis. An error of 1° in determining δ_4^F , however, has a somewhat larger effect on the coefficients. If $\delta_4^F=4^\circ$ is used, $a_5=0.089$, $a_3\approx 0.336$, $a_1\approx 1.025$, and the errors $\Delta a_5=-0.010$, $\Delta a_3=+0.020$, $\Delta a_1=+0.010$ are of the order of, but still smaller than, the least squares errors.

The sets of triplet phase shifts obtained from the polarization analysis were then used to calculate the differential cross section. Values of the singlet phase shifts K_0 and K_2 to be tried were obtained by choosing points on the ellipse determined by

$$\sin^2 K_0 + 5 \sin^2 K_2$$

$$= k^2 \left[4 \text{ mb} - \frac{1}{k^2} \sum_{L=1,3; J=0 \dots 4} (2J+1) \sin^2 \delta_J^L \right].$$

This also allows some limits to be set on the absolute value of K_2 . If all other phase shifts were zero, then a total cross section of $4\pi \times 4$ mb allows a $|K_2| \leq 33^\circ$. However, when triplet phase shifts determined by the polarization are used, the largest value of $|K_2|$ allowed in the present work was 14° . For the sets of phase shifts giving the best fits to data including interference, the

largest $|K_2|$ is only 7° . These limits may be useful in assessing results of phase shift calculations from assumed nucleon-nucleon interactions.

The cross section was calculated using a program prepared for the UNIVAC facility at New York University. The amplitudes as defined by Breit and Hull⁹ were first obtained, and the cross section computed from them according to formulas given by these authors. In addition, the polarization was calculated from the same amplitudes according to the formulas of Breit, Ehrman, and Hull.¹⁰ This latter calculation served both to check the polarization analysis and to obtain the effect of Coulomb interference at angles where it is important.

In the calculation of Coulomb effects, the value of the parameter η was obtained by using the relativistic formula of Garren and Breit¹¹:

$$\eta_{\text{rel}} = \left[\frac{(e^2/\hbar c)(1 + T_{\text{lab}}/Mc^2)}{[(T_{\text{lab}}/Mc^2)(2 + T_{\text{lab}}/Mc^2)]^{1/2}} \right].$$

Estimates using the results of Breit¹¹ and of Ebel and Hull¹² have indicated that the principal effect of treating the Coulomb interaction relativistically is contained simply in the changed value of η for energies under consideration.

The UNIVAC program allowed a comparison of theoretical and experimental angular distributions to be made by providing for the computation of

$$D = \sum_i \rho(\theta_i) \left| \frac{\sigma_{\text{exp}}(\theta_i) - \sigma_{\text{theor}}(\theta_i)}{\sigma_{\text{exp}}(\theta_i)} \right|,$$

where $\rho(\theta_i)$ is a weight assigned to an experimental value of the cross section at a given angle, θ_i . The cross-section data of Chamberlain *et al.*⁸ were used for comparison, with $\sigma(\theta)=3.75$ mb used for $\theta > 25^\circ$. For σ_{theor} differing from σ_{exp} by the experimental uncertainty at every angle, the value of D is about 0.6. Values of $(P\sigma)$ and σ , together with singlet and triplet cross sections and amplitudes were printed out at nine angles for all sets of phase shifts for the $D \leq 1$, and the value of D was printed for every set tried (about 1700).

Sample results of the calculation are shown in the accompanying figures. Figure 1 shows the data of Chamberlain *et al.*⁸ used for fitting together with curves representing the data. The data of Chamberlain and Garrison¹³ at 260 Mev are shown for comparison. The polarization curve is the result of a least squares analysis of data for $\theta > 25^\circ$, and is arbitrarily continued to smaller angles without including Coulomb interference. Theo-

⁹ G. Breit and M. H. Hull, Jr., Phys. Rev. **97**, 1047 (1955).

¹⁰ Breit, Ehrman, and Hull, Phys. Rev. **97**, 1051 (1955).

¹¹ G. Breit, Phys. Rev. **99**, 1581 (1955); see also A. Garren, Phys. Rev. **96**, 1709 (1954), where some similar results are given, but with insufficient justification to allow their general application in the present analysis.

¹² M. E. Ebel and M. H. Hull, Jr., Phys. Rev. **99**, 1596 (1955).

¹³ O. Chamberlain and J. D. Garrison, Phys. Rev. **95**, 1349 (1954).

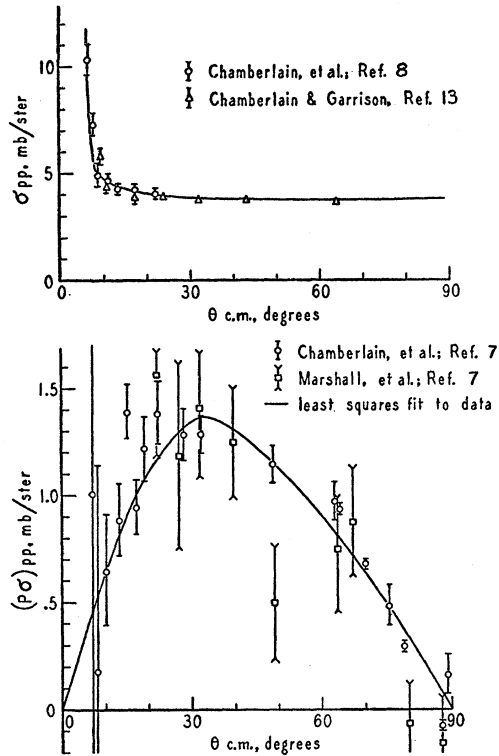


FIG. 1. Experimental data used in the present analysis. The upper curve shows the experimental points of Chamberlain *et al.*, reference 8, with other points due to Chamberlain and Garrison, reference 13, at 260 Mev shown for comparison. The curve is drawn through Chamberlain's experimental points, and extends to $\theta=90^\circ$ with the value $\sigma(\theta)=3.75$ mb/sterad to fit the average cross section of Chamberlain *et al.* in the second reference of footnote 8. The polarization curve represents a least squares fit to the data of Chamberlain *et al.* and of Marshall *et al.*, reference 7, for $\theta>25^\circ$, ignoring Coulomb interference. The curve is continued into the small-angle region using the same coefficients which fit the large-angle data.

retical curves are given in Figs. 2, 3, and 4 with the curves of Fig. 1 representing the data included for reference. The experimental points are omitted in the later figures for clarity. The phase shifts leading to the theoretical curves are given in Table I. Figure 2 contains some of the best cases found for both cross section and polarization. It is seen that while the cross section is represented fairly well below $\theta=10^\circ$ in these cases, the theoretical curve is not as flat as the experimental.

TABLE I. Sets of phase shifts resulting from the analysis which were used in calculating the differential cross sections and polarizations plotted in Figs. 2 and 3. Phase shifts are given in degrees. The letters at left refer to curve designations on Figs. 2 and 3.

	K_0	K_2	δ_0^P	δ_1^P	δ_2^P	δ_3^P	δ_4^P
A	-17.5	-4	-19.8	-19.8	20	10	-5
B	-3.75	-6	-38.5	-3.4	20	10	-10
C	0	0	-26.5	-19.7	19	10	-10
D	-30	-4	2.1	4.5	-15.5	0	-5
E	-2.5	-2	-33.6	-4.1	21	10	-5
F	35	0	16.6	9.6	2.2	-25	0

The calculated values of the polarization remain satisfactory fits to the data in these cases when the interference is included, even though they drop below the least squares curve. Figure 1 shows that the data scatter too much to rule them out.

The results in Fig. 3 illustrate some larger effects of Coulomb interference. Case *F* shows a strong negative interference in the polarization which is apparent even at $\theta=60^\circ$, although the effect is hardly experimentally significant at this angle. Case *D* shows a similarly strong positive interference. Both cases have one large 3F phase shift which accounts for much of the small-angle effect, while one large 3P phase shift sustains the effect at larger angles. Case *E* shows relatively small interference effects in the polarization except at very small angles.

The possibility of reducing the interference effects in cases *D* and *F* without changing the phase shifts by large amounts was investigated. Since the 3F phase shifts produce most of the effect, their contribution to the interference was to be eliminated while $a_6=0.099$ was to be held fixed. In both cases a first-order calculation produced such large changes in the phase shifts as to invalidate first-order considerations. Starting with the phase shifts in line *F* of Table I, it was found that changes $\Delta\delta_4^F=\pm 20^\circ$, $\Delta\delta_3^F=\pm 1^\circ$ were indicated in one arrangement of the calculation, and changes

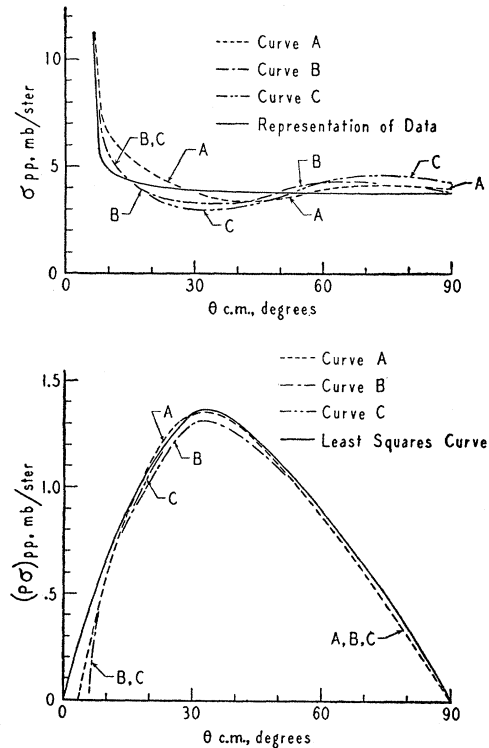


FIG. 2. Curves showing some of the fits obtained in the present analysis. The designations A, B, C represent different sets of phase shifts as given in Table I. The solid curves are the same as those of Fig. 1.

$\Delta\delta_4^F = 5^\circ$, $\Delta\delta_2^F = 32^\circ$ were indicated in another. When the phase shifts were initially those in line *D* of Table I, changes $\Delta\delta_2^F = \pm 19^\circ$, $\Delta\delta_4^F = \pm 47^\circ$, $\Delta\delta_6^F = \mp 14^\circ$ were indicated. In another case, to check the method, the phase shifts in line *E* of Table I were used, and the much smaller initial interference was reduced by changes $\Delta\delta_4^F = 2^\circ$, $\Delta\delta_6^F = 1.3^\circ$, $\Delta\delta_2^F = -2.9^\circ$, with a_5 kept constant.

It should be pointed out that these large changes occur in a special way of treating the effects. The data are not precise enough to determine a_5 exactly, so the requirement that a_5 remain unchanged is stringent. In addition, the spread of the data at small angles is so great that even for the two extreme cases under consideration the elimination of the effect of the 3P phase shifts cannot be said to be demanded by experiment. The main reason for discussing the interference effects at such length is to indicate that they can be relatively large: as much as 0.5–0.8 mb/sterad in $P\sigma$ for the special cases discussed. When experiments are improved, therefore, the interference effects can prove a useful tool in helping to determine suitable sets of phase shifts. At present, the existence of these extreme cases

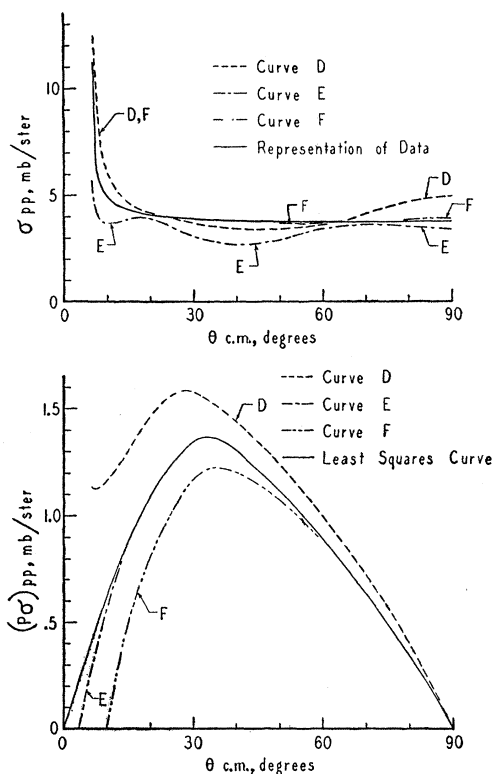


FIG. 3. Curves showing special interference effects. The designations *D*, *E*, *F* correspond to the sets of phase shifts so labeled in Table I. In the cross section, curves *D* and *F* start together at small angles, and *F* is essentially the same as the curve representing the data beyond $\theta = 20^\circ$. In the polarization, curve *E* joins the least squares curve at $\theta = 15^\circ$ and is not distinguishable from it at larger angles. The solid curves are the same as those of Fig. 1.

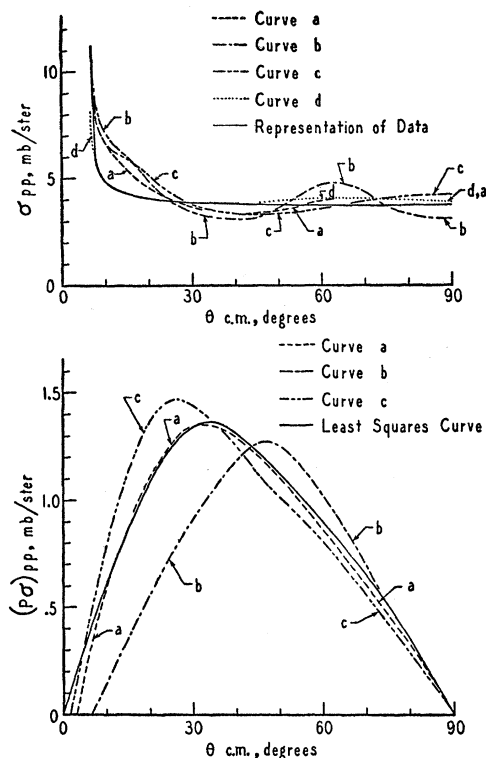


FIG. 4. Curves representing the effect of higher phase shifts. The curves labeled *a* are the same as those labeled *A* in Fig. 2 and correspond to the phase shifts of row *A* in Table I. For curves *b*, a phase shift $\delta_4^H = 3^\circ$ was added; for curves *c*, phase shifts $\delta_4^H = 0.5^\circ$, $\delta_5^H = 1^\circ$, $\delta_6^H = 1.5^\circ$ were added; for curve *d* (cross section only), the triplets were unchanged, but a singlet phase shift K_4 in the 1G_4 state was added. As the dotted line shows, curve *d* diverges slightly from the curve representing the data below 7° and above 45° , but is, on this scale, coincident with it in between. The solid curves are the same as those of Fig. 1.

suggests that the effects should be checked for any fits to data obtained without taking interference into account.

Case *F* produces the flattest cross section obtained in this analysis at large angles, fits the experimental curve well down to $\theta = 15^\circ$, but then rises too rapidly below this angle. This rise is due to Coulomb interference in the triplet cross section. Case *D* fits the experimental point at $\theta = 6.5^\circ$, but is very poor at $\theta = 90^\circ$. Case *E* shows a dip in cross section at $\theta = 10^\circ$, and does not show the experimental rise at smaller angles since the interference is too small in both singlet and triplet cross sections. The broad dip between 30° and 60° is, of course, an effect of the nuclear phase shifts rather than a Coulomb effect.

The effect of states with higher angular momentum was investigated by introducing small 1G and 3H phase shifts, to be used with the phase shifts of case *A*. Figure 4 represents the results, where curve *a* is the same as curve *A* of Fig. 2; for curve *b* the same 1S , 3P , 1D , 3F phase shifts as for curve *a* were used, with $\delta_4^H = 3^\circ$, $\delta_6^H = \delta_6^H = 0$; for curve *c* the 3H phase shifts

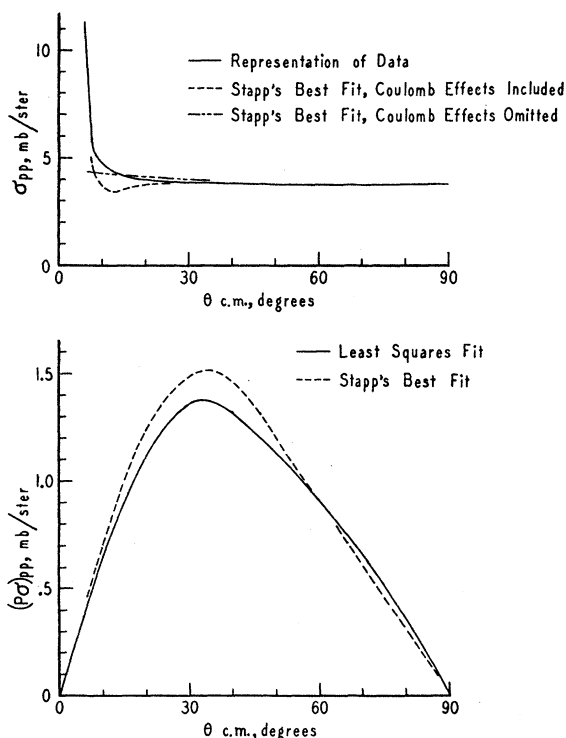


FIG. 5. Curves representing Stapp's best fit. In the polarization curve, the results with and without Coulomb interference are indistinguishable. In the cross-section curves, the dashed curve showing a dip at $\theta=10^\circ$ was calculated including interference. The dashed curve showing no dip was calculated without interference. The solid curves are the same as those of Fig. 1.

were changed to $\delta_4^H=0.5^\circ$, $\delta_6^H=1^\circ$, $\delta_8^H=1.5^\circ$; for curve *d* the 3H phase shifts were zero as for curve *a*, and $\delta_4^G=3^\circ$ was used. Inspection of the polarization curves shows that the relatively large $\delta_4^H=3^\circ$ used for curve *b* has the same effect as the large $\delta_2^F=-25^\circ$ of case *F* of Fig. 3, while $\delta_6^H=1.5^\circ$ used for curve *c* produces an effect somewhat like that found for $\delta_4^F=16.3^\circ$ of case *D* of Fig. 3. Both sets of 3H phase shifts produce a larger angular variation of the differential cross section than that of curve *a*, while the introduction of a positive 1G phase shift improved the angular dependence quite a bit, although the extent of the small-angle rise is not reproduced because the Coulomb interference is cut down in the singlet cross section.

In the course of the analysis of the results of the UNIVAC calculations, another discussion of the proton-proton data at 300 Mev in terms of phase shifts appeared.¹⁴ In this work, Stapp has used a gradient

method to fit σ , $P\sigma$, and some of the triple-scattering parameters by means of S , P , D , and F phase shifts and the coupling between P and F states. The cross section and polarization resulting from what he calls his best fit were recalculated here, including Coulomb effects, and are shown in Fig. 5. This fit gives $K_0=-35.1^\circ$, $K_2=1.83^\circ$, $\delta_0^P=-25.6^\circ$, $\delta_1^P=-8.88^\circ$, $\delta_2^P=23.1^\circ$, $\delta_2^F=-2.23^\circ$, $\delta_3^F=0.92^\circ$, $\delta_4^F=3.55^\circ$, and the coupling parameter is $\epsilon=-15.6^\circ$. Stapp did not include Coulomb effects except to see that the interference in the cross section at $\theta=10^\circ$ corresponded to an experimental result privately communicated by Ypsilantis. In Fig. 5 it is seen that Stapp's phase shifts lead to a dip in the cross section at small angles when Coulomb effects are included, and that the rise at smaller angles is less than that exhibited by the data used in the present analysis. Although the data of Chamberlain *et al.*⁸ do not show the dip, data at higher energies indicate it,¹⁵ and Stapp presumably had later information at 300 Mev. Coulomb effects on the polarization are negligible at all angles above 7° for Stapp's phase shifts. His polarization curve, as shown in Fig. 5, appears to peak more sharply than the data. The difference may not be significant in view of the uncertainties in the experimental points. Thus Stapp's best fit is more satisfactory than fits so far obtained in the present work in that he has reproduced both the flatness of the cross section at large angles and the shape of the polarization curve over most of the experimental angular range, and has also included other types of data in his analysis. At small angles, however, the cross section leaves something to be desired.

The figures illustrate the advantages of supplementing the results of any method of analysis with a comparison of experimental and theoretical curves. A judgment as to the value of a given set of phase shifts is more readily made when such a comparison is available. The importance of including Coulomb interference effects in the analysis are also brought out clearly by this means.

ACKNOWLEDGMENTS

The authors wish to express their appreciation to Professor G. Breit, who planned much of the work and suggested the methods used in carrying it out. They also wish to thank the U. S. Atomic Energy Commission for making possible the use of the New York University UNIVAC facility, and the staff of that facility for their cooperation. The courtesy of Mr. H. P. Stapp in allowing his results to be used before publication is appreciated.

¹⁴ H. P. Stapp, University of California Radiation Laboratory Report UCRL-3098 (unpublished).

¹⁵ D. Fischer and G. Goldhaber, Phys. Rev. **99**, 1350 (1955).